Chemistry–A European Journal

Supporting Information

Chemical Bonding in Homoleptic Carbonyl Cations $[M\{Fe(CO)_5\}_2]^+$ (M = Cu, Ag, Au)

Sudip Pan,[a, b] Sai Manoj N. V. T. Gorantla,[b] Devaborniny Parasar,[c] H. V. Rasika Dias,*[c] and Gernot Frenking*[a, b]

Theoretical Methods

The geometry optimization followed by the vibrational frequencies calculations were performed at the BP86-D3(BJ)/def2-TZVPP level.[1] All calculated complexes are minima on the potential energy surfaces as understood by the absence of any imaginary frequency. All these calculations were carried out with Gaussian 16 program package.[2] The natural bond orbital (NBO) analysis[3] were performed to evaluate the partial charge using NBO 6.0 program.[4] The quantum theory of atoms in molecules analysis[5] was done with the AIMALL program[6] at the BP86-D3(BJ)/def2TZVPP/x2C-TZVPall[7] where all-electron x2C-TZVPall basis set was used for Ag and Au atoms.

The bonding situations were analyzed by means of an energy decomposition analysis (EDA)[8] together with the natural orbitals for chemical valence (NOCV)[9] method by using the ADF 2018.105 program package.[10] The EDA-NOCV calculations were carried out at the BP86-D3(BJ)/TZ2P-ZORA level[11] using the BP86-D3(BJ)/def2-TZVPP optimized geometries. In this analysis, the intrinsic interaction energy (ΔE_{int}) between two fragments can be divided into three energy components as follows:

$$\Delta E_{\text{int}} = \Delta E_{\text{elstat}} + \Delta E_{\text{Pauli}} + \Delta E_{\text{orb}} + \Delta E_{\text{disp}} \qquad (1).$$

While the electrostatic ΔE_{elstat} term represents the quasiclassical electrostatic interaction between the unperturbed charge distributions of the prepared fragments, the Pauli repulsion ΔE_{Pauli} corresponds to the energy change associated with the transformation from the superposition of the unperturbed electron densities of the isolated fragments to the wavefunction, which properly obeys the Pauli principle through explicit antisymmetrization and renormalization of the production wavefunction. Since we included D3(BJ), it provides us with the dispersion interaction energy between two interacting fragments. The orbital term ΔE_{orb} is originated from the mixing of orbitals, charge transfer and polarization between the isolated fragments, which can be further decomposed into contributions from each irreducible representation of the point group of the interacting system as follows:

$$\Delta E_{orb} = \sum_{r} \Delta E_{r} \qquad (2)$$

The combination of the EDA with NOCV enables the partition of the total orbital interactions into pairwise contributions of the orbital interactions which is very vital to get a

complete picture of the bonding. The charge deformation $\Delta\rho_k(r)$, resulting from the mixing of the orbital pairs $\psi_k(r)$ and $\psi_{-k}(r)$ of the interacting fragments presents the amount and the shape of the charge flow due to the orbital interactions (Equation 3), and the associated energy term ΔE_{orb} provides with the size of stabilizing orbital energy originated from such interaction (Equation 4).

$$\Delta\rho_{orb}(r) = \sum_k \Delta\rho_k(r) = \sum_{k=1}^{N/2} \nu_k [-\psi_{-k}^2(r) + \psi_k^2(r)] \qquad (3)$$

$$\Delta E_{orb} = \sum_k \Delta E_k^{orb} = \sum_{k=1}^{N/2} \nu_k [-F_{-k,-k}^{TS} + F_{k,k}^{TS}] \qquad (4)$$

More details about the EDA-NOCV method and its application are given in recent reviews articles.[12]

Experimental Methods

Experimental Procedures

All manipulations were carried out under an atmosphere of purified nitrogen using standard Schlenk techniques. Solvents were purchased from commercial sources and purified by conventional methods prior to use. Glassware was oven-dried at 150°C overnight. IR spectra were collected at room temperature on a Shimadzu IRPrestige-21 FT-IR containing an ATR attachment at 2 cm^{-1} resolution. The $AgSbF_6$ was purchased from Sigma-Aldrich Company and was used as received. $Fe(CO)_5$ was obtained from Sigma-Aldrich Company and distilled prior to use. The $[M\{Fe(CO)_5\}_2][SbF_6]$ (M = Cu, Ag, Au) compounds have been prepared following reported procedures.[13]

$[Cu\{Fe(CO)_5\}_2][SbF_6]$: The CuBr (0.150 g, 1.05 mmol) and $AgSbF_6$ (0.361 g, 1.05 mmol) were placed in a flask with a magnetic stir bar. Dichloromethane (~12 mL) saturated with ethylene, and this solution was added to the mixture at room temperature. The mixture was stirred for about 3 hours under ethylene atmosphere. Ethylene was gently bubbled into the mixture (3 x 5 min) during this period to maintain an ethylene rich solution. A yellow-greenish precipitate (AgBr) was formed over time, which was removed by filtration through Celite. The resulting solution of $[Cu(C_2H_4)_3][SbF_6]$ was concentrated to about 3 mL using ethylene. A yellow solution of $Fe(CO)_5$ (0.514 g, 2.63 mmol) in dichloromethane (1 mL) was added dropwise to $[Cu(C_2H_4)_3][SbF_6]$ (considering 100% conversion) solution at -70 °C. The resulting pale-yellow solution was stirred for ~15 mins, and hexane (~2 mL) was added. Finally, the solution was filtered and kept at -20 °C overnight to obtain $[Cu\{Fe(CO)_5\}_2][SbF_6]$ as colorless crystals. ATR-IR (single crystals, ν_{CO}, cm^{-1}): 2131 (m), 2084 (m sh), 2031 (vs), 1997 (s).

$[Ag\{Fe(CO)_5\}_2][SbF_6]$: A yellow solution of $Fe(CO)_5$ (0.284 g, 1.45 mmol) in dichloromethane (1-2 mL) was added dropwise to $AgSbF_6$ (200 mg, 0.58 mmol) in dichloromethane (~6 mL) at -70 °C. The resulting pale-yellow solution was stirred for 10 min and kept at -20 °C overnight to obtain $[Ag\{Fe(CO)_5\}_2][SbF_6]$ as colorless crystals. ATR-IR (single crystals, cm^{-1}): 2127, 2051, 2016. The $[Ag\{Fe(CO)_5\}_2][SbF_6]$ can also be isolated from

in-situ generated $[Ag(C_2H_4)_3][SbF_6]$ and $Fe(CO)_5$. $AgSbF_6$ (0.120 g, 0.35 mmol) was placed in a flask with a magnetic stir bar. Dichloromethane (~10 mL) saturated with ethylene was added to the mixture at room temperature. The mixture was stirred for about 2 hours under ethylene atmosphere. Ethylene was gently bubbled into the mixture (3 x 4 min) during this period to maintain an ethylene rich solution. The resulting solution of $[Ag(C_2H_4)_3][SbF_6]$ was concentrated to about 3 mL by bubbling ethylene, and then slowly cooled down to -70 °C. A solution of $Fe(CO)_5$ (0.171 g, 0.88 mmol, calculated considering 100% conversion of $AgSbF_6$ to $[Ag(C_2H_4)_3][SbF_6]$) in dichloromethane (1-2 mL) was added to it dropwise. The resulting reaction mixture was stirred for ~10 min and kept in refrigerator at -20 °C to obtain $[Ag\{Fe(CO)_5\}_2][SbF_6]$ as colorless crystals. The complex can be isolated as crystalline white solid (by purging with nitrogen). Upon exposure to air the white solid becomes sticky, and slowly changes color to black. ATR-IR (single crystals, ν_{CO}, cm^{-1}): 2127 (m), 2051 (s), 2016 (vs).

$[Au\{Fe(CO)_5\}_2][HOB\{3,5\text{-}(CF_3)_2C_6H_3\}_3]$: AuCl (0.100 g, 0.43 mmol) and $Na[B\{3,5\text{-}(CF_3)_2C_6H_3\}_4]$ (0.381 g, 0.43 mmol) were placed in a flask with a magnetic stir bar. Dichloromethane (~10 mL) saturated with ethylene was added to the mixture at room temperature. The mixture was stirred for about 3 hours under ethylene atmosphere. Ethylene was gently bubbled into the mixture (3 x 5 min) during this period to maintain an ethylene rich solution. A precipitate (NaCl) was formed over time, which was removed by filtration through Celite. The resulting filtrate was concentrated to ~3 mL by bubbling ethylene. A yellow solution of $Fe(CO)_5$ (0.211 g, 1.08 mmol) in dichloromethane (1-2 mL) was added dropwise to $Au(C_2H_4)_3[B\{3,5\text{-}(CF_3)_2C_6H_3\}_4]$ (considering 100 % conversion) solution at -70 °C. The resulting black solution was stirred for ~10 mins and mixed with some hexane and kept in refrigerator at -20 °C. A white powder was obtained, $[Au\{Fe(CO)_5\}_2][B\{3,5\text{-}(CF_3)_2C_6H_3\}_4]$. ATR-IR (solid powder, ν_{CO}, cm^{-1}): 2133 (m), 2084 (vs), 2070 (s), 2053 (vs). The mixture was filtered while maintaining the cold temperature and the filtrate was kept in a cold freezer (-20 °C) to obtain crystals of $[Au\{Fe(CO)_5\}_2][HOB\{3,5\text{-}(CF_3)_2C_6H_3\}_3]$. ATR-IR (single crystals, ν_{CO}, cm^{-1}): 2131 (m), 2069 (vs).

Summary of IR data

	$\bar{\upsilon}_{CO}$ (cm^{-1})
$Cu\{Fe(CO)_5\}_2FSbF_5$	2131 (m), 2084 (m, sh), 2031 (vs), 1997 (s)
$[Ag\{Fe(CO)_5\}_2][SbF_6]$	2127 (m), 2051 (s), 2016 (vs)
$[Au\{Fe(CO)_5\}_2][SbF_6]$ – powder and micro crystals	2128 (m) , 2060 (vs br), 2037 (vs)
$[Au\{Fe(CO)_5\}_2][B\{3,5\text{-}(CF_3)_2C_6H_3\}_4]$ – solid powder	2133 (m), 2084 (vs), 2070 (s), 2053 (vs)
$[Au\{Fe(CO)_5\}_2][HOB\{3,5\text{-}(CF_3)_2C_6H_3\}_3]$ - crystals	2131 (m), 2069 (s)
Free $Fe(CO)_5$	2024, 2000

X-ray Data Collection and Structure Determinations

A suitable crystal covered with a layer of hydrocarbon/Paratone-N oil was selected and mounted on a Cryo-loop, and immediately placed in the low temperature nitrogen stream. The X-ray intensity data were measured at 100(2) K (unless otherwise noted) on a Bruker D8 Quest with a Photon 100 CMOS detector equipped with an Oxford Cryosystems 700 series cooler, a Triumph graphite monochromator, and a Mo Kα fine-focus sealed tube (λ = 0.71073 Å). Intensity data were processed using the Bruker Apex program suite. Absorption corrections were applied by using SADABS.[14] Initial atomic positions were located by SHELXT,[15] and the structures of the compounds were refined by the least-squares method using SHELXL[16] within Olex2 GUI.[17] All the non-hydrogen atoms were refined anisotropically. The H atoms were included in their calculated positions and refined as riding on the atoms to which they are joined. X-ray structural figures were generated using Olex2.[17] The CCDC 1999550, 1999551 and 2027017 contain the supplementary crystallographic data for these molecules.

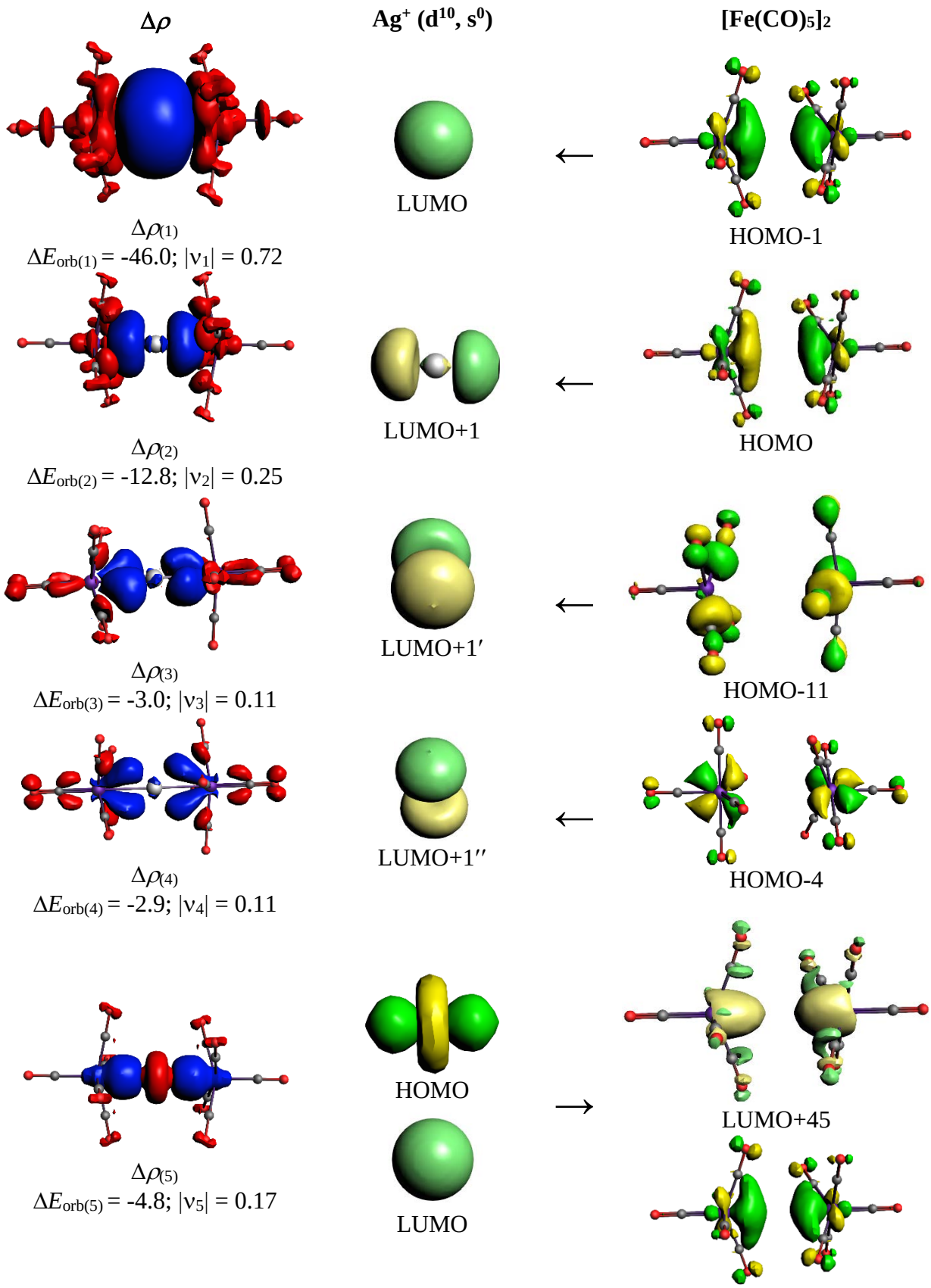
Δρ
Ag+ (d10, s0)
[Fe(CO)5]2
LUMO
HOMO-1
Δρ(1)
ΔEorb(1) = -46.0; |ν1| = 0.72
LUMO+1
HOMO
Δρ(2)
ΔEorb(2) = -12.8; |ν2| = 0.25
LUMO+1′
HOMO-11
Δρ(3)
ΔEorb(3) = -3.0; |ν3| = 0.11
LUMO+1″
HOMO-4
Δρ(4)
ΔEorb(4) = -2.9; |ν4| = 0.11
HOMO
LUMO+45
Δρ(5)
ΔEorb(5) = -4.8; |ν5| = 0.17
LUMO

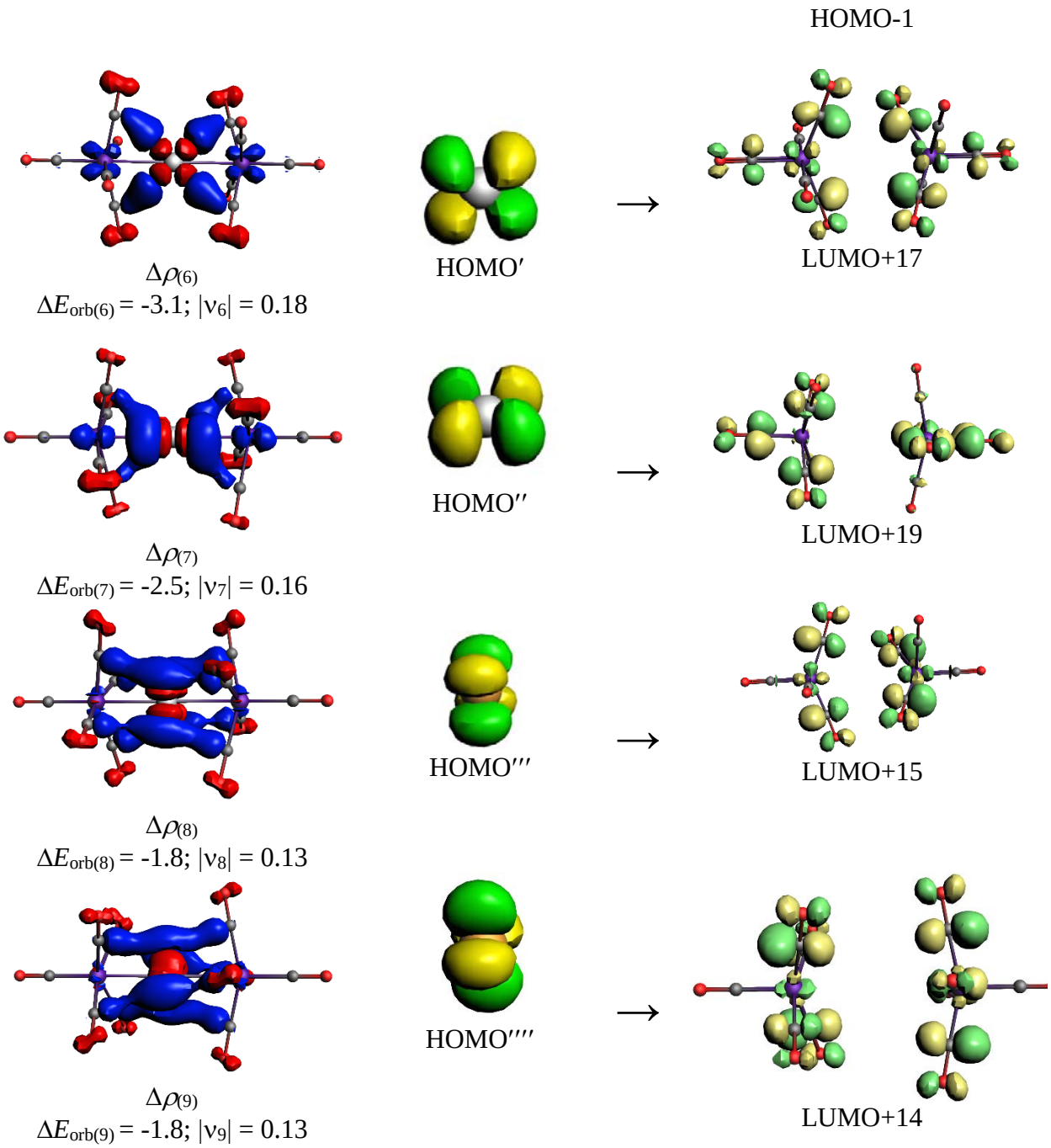

Figure S1. The shape of the deformation densities, $\Delta\rho_{(1)\text{-}(9)}$ which are associated with $\Delta E_{\text{orb}(1)\text{-}(9)}$, and the most important associated fragment orbitals for $[Ag\{Fe(CO)_5\}_2]^+$ at the BP86-D3(BJ)/TZ2P-ZORA//BP86-D3(BJ)/def2-TZVPP level. The isovalue is 0.0004 au for $\Delta\rho_{(1)\text{-}(2)}$ and 0.0002 au for the rest. The eigenvalues υ give the size of the charge migration. The direction of the charge flow of the deformation densities is red→blue.

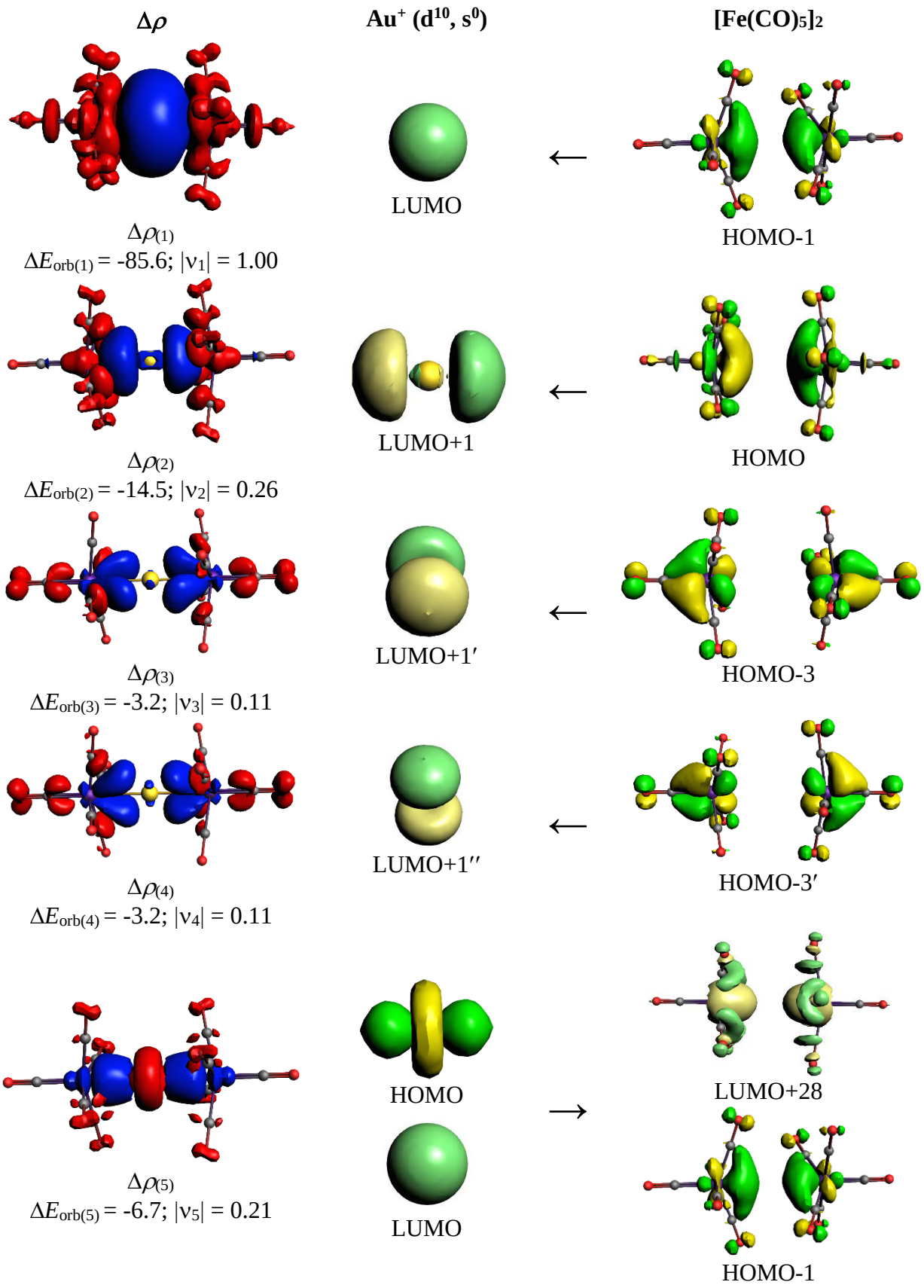
Δρ
Au+ (d10, s0)
[Fe(CO)5]2
LUMO
HOMO-1
Δρ(1)
ΔEorb(1) = -85.6; |ν1| = 1.00
LUMO+1
HOMO
Δρ(2)
ΔEorb(2) = -14.5; |ν2| = 0.26
LUMO+1′
HOMO-3
Δρ(3)
ΔEorb(3) = -3.2; |ν3| = 0.11
LUMO+1″
HOMO-3′
Δρ(4)
ΔEorb(4) = -3.2; |ν4| = 0.11
HOMO
LUMO+28
Δρ(5)
ΔEorb(5) = -6.7; |ν5| = 0.21
LUMO
HOMO-1

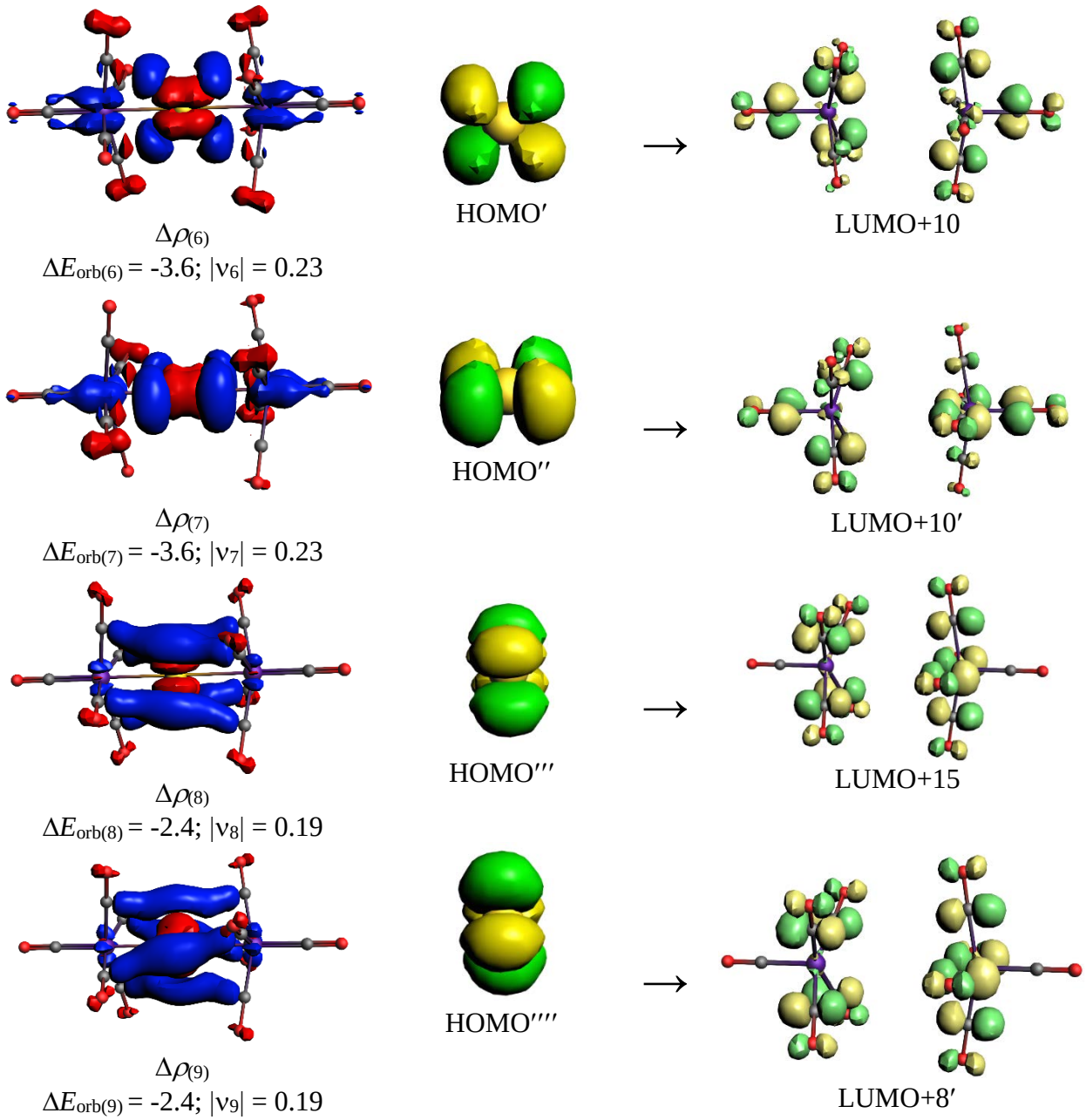

Figure S2. The shape of the deformation densities, $\Delta\rho_{(1)\text{-}(9)}$ which are associated with $\Delta E_{\text{orb}(1)\text{-}(9)}$, and the most important associated fragment orbitals for $[Au\{Fe(CO)_5\}_2]^+$ at the BP86-D3(BJ)/TZ2P-ZORA//BP86-D3(BJ)/def2-TZVPP level. The isovalue is 0.0004 au for $\Delta\rho_{(1)\text{-}(2)}$ and 0.0002 au for the rest. The eigenvalues υ give the size of the charge migration. The direction of the charge flow of the deformation densities is red→blue.

Table S1. Relative energies (E_{rel}, kcal/mol) of different conformations of $[M\{Fe(CO)_5\}_2]^+$ (M = Cu, Ag, Au) complexes at the BP86-D3(BJ)/def2-TZVPP level.

	E_{rel}, kcal/mol		
	(D_2, ^1A)	(D_4, $^1A_1$)	(D_{4d}, $^1A_1$)
$Cu[Fe(CO)_5]_2^+$	0.0	1.8 (43.6*i*, 36.6*i*, 8.6*i*)	1.5 (45.6*i*, 45.6*i*)
$Ag[Fe(CO)_5]_2^+$	0.0	0.1 (10.9*i*, 8.2*i*, 4.3*i*)	0.01 (10.9*i*, 10.6*i*)
$Au[Fe(CO)_5]_2^+$	-a-	0.1 (3.8*i*)	0.0

[a]D_2 structure collapse to the D_{4d} geometry during geometry optimization.

Table S2. Energies and coordinates of the calculated molecules at the BP86-D3(BJ)/def2-TZVPP level.

$[Cu\{Fe(CO)_5\}_2]^+$ (D_2, ^1A) E = -5302.621907 au 1 1 Fe 0.00000000 0.00000000 2.40131700 O -2.41762400 1.41761500 1.40465500 O -1.50259200 -2.56198900 2.41030300 O 0.00000000 0.00000000 5.37106300 O 1.50259200 2.56198900 2.41030300 O 2.41762400 -1.41761500 1.40465500 C -0.92444800 -1.57539500 2.40017900 C -1.47287200 0.86319300 1.76108000 C 0.00000000 0.00000000 4.22756800 C 1.47287200 -0.86319300 1.76108000 C 0.92444800 1.57539500 2.40017900 Fe 0.00000000 0.00000000 -2.40131700 O 2.41762400 1.41761500 -1.40465500 O -1.50259200 2.56198900 -2.41030300 O 0.00000000 0.00000000 -5.37106300 O 1.50259200 -2.56198900 -2.41030300 O -2.41762400 -1.41761500 -1.40465500 C -0.92444800 1.57539500 -2.40017900 C 1.47287200 0.86319300 -1.76108000 C 0.00000000 0.00000000 -4.22756800 C -1.47287200 -0.86319300 -1.76108000 C 0.92444800 -1.57539500 -2.40017900 Cu 0.00000000 0.00000000 0.00000000
$[Cu\{Fe(CO)_5\}_2]^+$ (D_4, $^1A_1$) E = -5302.618993 au 1 1 Fe 0.00000000 0.00000000 2.39522900 O 0.02902300 2.92669800 1.89192800 O -2.92669800 0.02902300 1.89192800 O 0.00000000 0.00000000 5.37410700 O 2.92669800 -0.02902300 1.89192800 O -0.02902300 -2.92669800 1.89192800 C -1.79626200 0.01778100 2.08381100 C 0.01778100 1.79626200 2.08381100 C 0.00000000 0.00000000 4.23173200

C -0.01778100 -1.79626200 2.08381100 C 1.79626200 -0.01778100 2.08381100 Fe 0.00000000 0.00000000 -2.39522900 O 0.02902300 -2.92669800 -1.89192800 O 2.92669800 0.02902300 -1.89192800 O 0.00000000 0.00000000 -5.37410700 O -2.92669800 -0.02902300 -1.89192800 O -0.02902300 2.92669800 -1.89192800 C 1.79626200 0.01778100 -2.08381100 C 0.01778100 -1.79626200 -2.08381100 C 0.00000000 0.00000000 -4.23173200 C -0.01778100 1.79626200 -2.08381100 C -1.79626200 -0.01778100 -2.08381100 Cu 0.00000000 0.00000000 0.00000000
$[Cu\{Fe(CO)_5\}_2]^+$ (D_{4d}, $^1A_1$) E = -5302.619446 au 1 1 Fe 0.00000000 0.00000000 2.39028700 O 0.00000000 2.92285800 1.86354100 O -2.92285800 0.00000000 1.86354100 O 0.00000000 0.00000000 5.36842000 O 2.92285800 0.00000000 1.86354100 O 0.00000000 -2.92285800 1.86354100 C -1.79450800 0.00000000 2.06833400 C 0.00000000 1.79450800 2.06833400 C 0.00000000 0.00000000 4.22603300 C 0.00000000 -1.79450800 2.06833400 C 1.79450800 0.00000000 2.06833400 Fe 0.00000000 0.00000000 -2.39028700 O 2.06677300 -2.06677300 -1.86354100 O 2.06677300 2.06677300 -1.86354100 O 0.00000000 0.00000000 -5.36842000 O -2.06677300 -2.06677300 -1.86354100 O -2.06677300 2.06677300 -1.86354100 C 1.26890900 1.26890900 -2.06833400 C 1.26890900 -1.26890900 -2.06833400 C 0.00000000 0.00000000 -4.22603300 C -1.26890900 1.26890900 -2.06833400 C -1.26890900 -1.26890900 -2.06833400 Cu 0.00000000 0.00000000 0.00000000
$[Ag\{Fe(CO)_5\}_2]^+$ (D_2, ^1A)

E = -3808.935510 au

1 1
Fe 0.00000000 0.00000000 2.59724600
O -1.13661300 -2.72522900 2.27389300
O 2.69301000 -1.12335600 2.03354500
O 0.00000000 0.00000000 5.56831500
O -2.69301000 1.12335600 2.03354500
O 1.13661300 2.72522900 2.27389300
C 1.65039300 -0.68824700 2.23316900
C -0.69804400 -1.67348600 2.38994700
C 0.00000000 0.00000000 4.42531400
C 0.69804400 1.67348600 2.38994700
C -1.65039300 0.68824700 2.23316900
Fe 0.00000000 0.00000000 -2.59724600
O -1.13661300 2.72522900 -2.27389300
O -2.69301000 -1.12335600 -2.03354500
O 0.00000000 0.00000000 -5.56831500
O 2.69301000 1.12335600 -2.03354500
O 1.13661300 -2.72522900 -2.27389300
C -1.65039300 -0.68824700 -2.23316900
C -0.69804400 1.67348600 -2.38994700
C 0.00000000 0.00000000 -4.42531400
C 0.69804400 -1.67348600 -2.38994700
C 1.65039300 0.68824700 -2.23316900
Ag 0.00000000 0.00000000 0.00000000

$[Ag\{Fe(CO)_5\}_2]^+$ (D_4, $^1A_1$)

E = -3808.935326 au

1 1
Ag 0.00000000 0.00000000 0.00000000
Fe 0.00000000 0.00000000 2.59757300
O 0.01810200 2.93804400 2.15667800
O -2.93804400 0.01810200 2.15667800
O 0.00000000 0.00000000 5.56894800
O 2.93804400 -0.01810200 2.15667800
O -0.01810200 -2.93804400 2.15667800
C -1.80262300 0.01106900 2.31375400
C 0.01106900 1.80262300 2.31375400
C 0.00000000 0.00000000 4.42595000
C -0.01106900 -1.80262300 2.31375400
C 1.80262300 -0.01106900 2.31375400
Fe 0.00000000 0.00000000 -2.59757300
O 0.01810200 -2.93804400 -2.15667800

O 2.93804400 0.01810200 -2.15667800
O 0.00000000 0.00000000 -5.56894800
O -2.93804400 -0.01810200 -2.15667800
O -0.01810200 2.93804400 -2.15667800
C 1.80262300 0.01106900 -2.31375400
C 0.01106900 -1.80262300 -2.31375400
C 0.00000000 0.00000000 -4.42595000
C -0.01106900 1.80262300 -2.31375400
C -1.80262300 -0.01106900 -2.31375400

$[Ag\{Fe(CO)_5\}_2]^+$ (D_{4d}, $^1A_1$)

E = -3808.935500 au

1 1
Ag 0.00000000 0.00000000 0.00000000
Fe 0.00000000 0.00000000 2.59530900
O 0.00000000 2.93756300 2.15148300
O -2.93756300 0.00000000 2.15148300
O 0.00000000 0.00000000 5.56665700
O 2.93756300 0.00000000 2.15148300
O 0.00000000 -2.93756300 2.15148300
C -1.80230400 0.00000000 2.30982300
C 0.00000000 1.80230400 2.30982300
C 0.00000000 0.00000000 4.42372200
C 0.00000000 -1.80230400 2.30982300
C 1.80230400 0.00000000 2.30982300
Fe 0.00000000 0.00000000 -2.59530900
O 2.07717000 -2.07717000 -2.15148300
O 2.07717000 2.07717000 -2.15148300
O 0.00000000 0.00000000 -5.56665700
O -2.07717000 -2.07717000 -2.15148300
O -2.07717000 2.07717000 -2.15148300
C 1.27442100 1.27442100 -2.30982300
C 1.27442100 -1.27442100 -2.30982300
C 0.00000000 0.00000000 -4.42372200
C -1.27442100 1.27442100 -2.30982300
C -1.27442100 -1.27442100 -2.30982300

$[Au\{Fe(CO)_5\}_2]^+$ (D_{4d}, $^1A_1$)

E = -3797.716800 au

1 1
Fe 0.00000000 0.00000000 2.57784500

O 0.00000000 2.94036800 2.13439300
O -2.94036800 0.00000000 2.13439300
O 0.00000000 0.00000000 5.54788700
O 2.94036800 0.00000000 2.13439300
O 0.00000000 -2.94036800 2.13439300
C -1.80688800 0.00000000 2.29511700
C 0.00000000 1.80688800 2.29511700
C 0.00000000 0.00000000 4.40496700
C 0.00000000 -1.80688800 2.29511700
C 1.80688800 0.00000000 2.29511700
Fe 0.00000000 0.00000000 -2.57784500
O 2.07915400 -2.07915400 -2.13439300
O 2.07915400 2.07915400 -2.13439300
O 0.00000000 0.00000000 -5.54788700
O -2.07915400 -2.07915400 -2.13439300
O -2.07915400 2.07915400 -2.13439300
C 1.27766300 1.27766300 -2.29511700
C 1.27766300 -1.27766300 -2.29511700
C 0.00000000 0.00000000 -4.40496700
C -1.27766300 1.27766300 -2.29511700
C -1.27766300 -1.27766300 -2.29511700
Au 0.00000000 0.00000000 0.00000000

$[Au\{Fe(CO)_5\}_2]^+$ (D_4, $^1A_1$)

E = -3797.716658 au

1 1
Fe 0.00000000 0.00000000 2.57919800
O 0.02038900 2.94112100 2.14100900
O -2.94112100 0.02038900 2.14100900
O 0.00000000 0.00000000 5.54980000
O 2.94112100 -0.02038900 2.14100900
O -0.02038900 -2.94112100 2.14100900
C -1.80733200 0.01250700 2.29964100
C 0.01250700 1.80733200 2.29964100
C 0.00000000 0.00000000 4.40687800
C -0.01250700 -1.80733200 2.29964100
C 1.80733200 -0.01250700 2.29964100
Fe 0.00000000 0.00000000 -2.57919800
O 0.02038900 -2.94112100 -2.14100900
O 2.94112100 0.02038900 -2.14100900
O 0.00000000 0.00000000 -5.54980000
O -2.94112100 -0.02038900 -2.14100900
O -0.02038900 2.94112100 -2.14100900
C 1.80733200 0.01250700 -2.29964100
C 0.01250700 -1.80733200 -2.29964100

C 0.00000000 0.00000000 -4.40687800
C -0.01250700 1.80733200 -2.29964100
C -1.80733200 -0.01250700 -2.29964100
Au 0.00000000 0.00000000 0.00000000

Figure S3. Molecular structure and atom numbering scheme for $[Cu\{Fe(CO)_5]_2[SbF_6]$**.** There are two chemically similar molecules in the asymmetric unit.

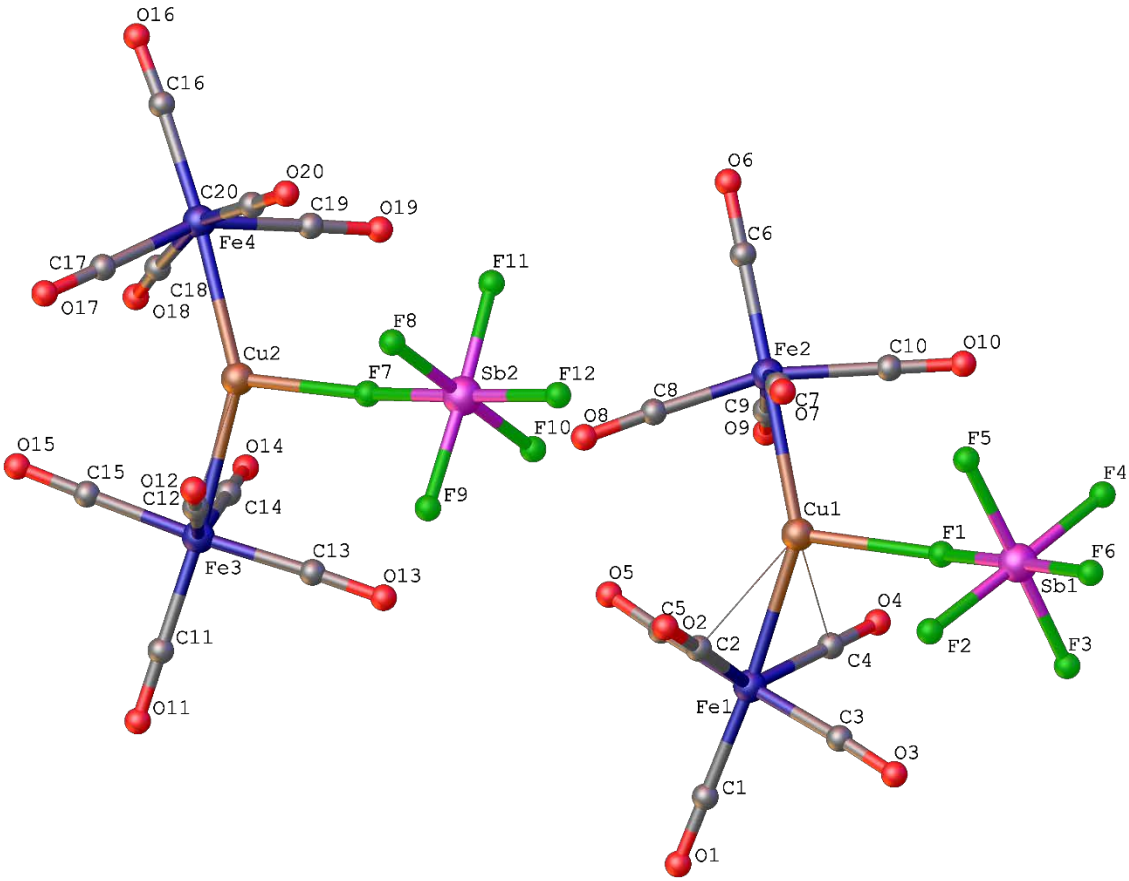

Table S3. Crystal data and structure refinement for $[Cu\{Fe(CO)_5]_2[SbF_6]$.

Identification code	RAD566
Empirical formula	$C_{10}CuF_6Fe_2O_{10}Sb$
Formula weight	691.09
Temperature/K	100.0
Crystal system	monoclinic
Space group	$P2_1/c$
a/Å	13.6737(10)
b/Å	22.3624(17)
c/Å	13.0401(10)
α/°	90
β/°	104.497(3)
γ/°	90
Volume/Å^3	3860.4(5)
Z	8
ρ_{calc}g/cm^3	2.378
μ/mm^{-1}	4.047
F(000)	2608.0
Crystal size/mm^3	0.42 × 0.32 × 0.035
Radiation	MoKα (λ = 0.71073)
2Θ range for data collection/°	6.156 to 52.998
Index ranges	$-17 \leq h \leq 17$, $-27 \leq k \leq 28$, $-16 \leq l \leq 16$
Reflections collected	18699
Independent reflections	7849 [R_{int} = 0.0512, R_{sigma} = 0.0901]
Data/restraints/parameters	7849/0/541
Goodness-of-fit on F^2	1.103
Final R indexes [I>=2σ (I)]	R_1 = 0.0695, wR_2 = 0.1535
Final R indexes [all data]	R_1 = 0.0981, wR_2 = 0.1712
Largest diff. peak/hole / e Å^{-3}	1.50/-1.84

Figure S4. Molecular structure and atom numbering scheme for $[Ag\{Fe(CO)_5\}_2][SbF_6]$.

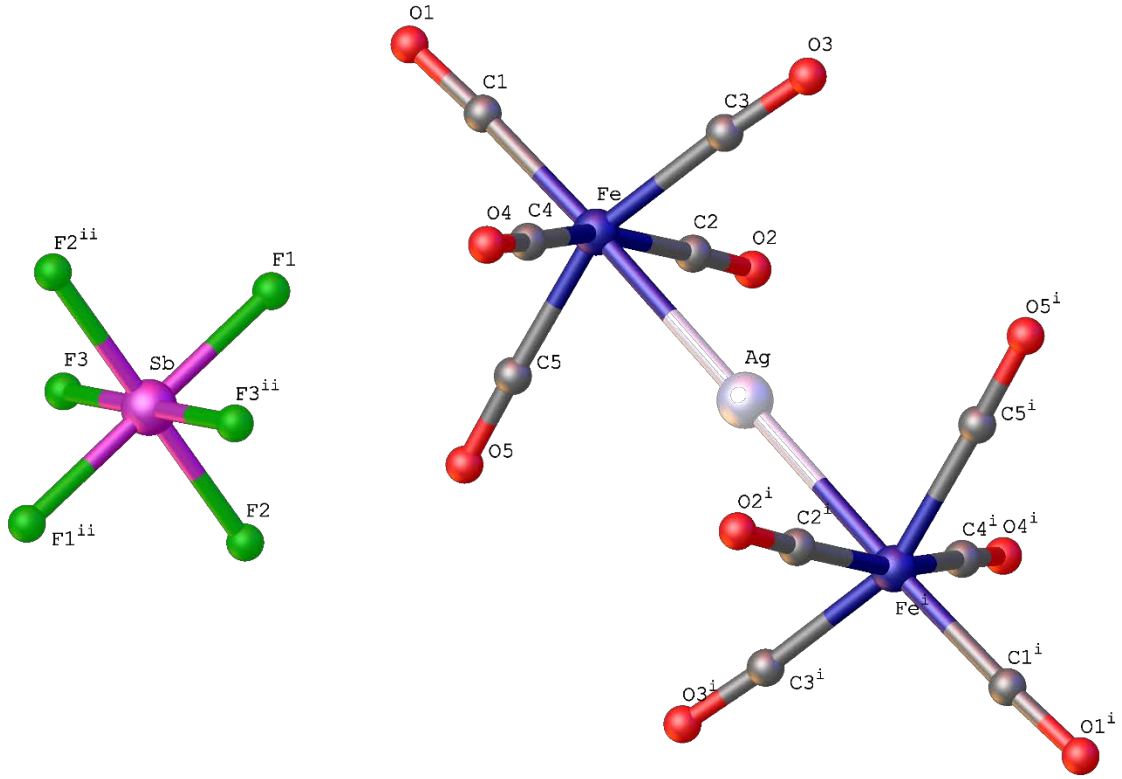

Table S4. Crystal data and structure refinement for $[Ag\{Fe(CO)_5\}_2][SbF_6]$.

Identification code	RAD562
Empirical formula	$C_{10}AgF_6Fe_2O_{10}Sb$
Formula weight	735.42
Temperature/K	100.0
Crystal system	monoclinic
Space group	$P2_1/n$
a/Å	6.3841(5)
b/Å	12.6173(9)
c/Å	11.3212(8)
α/°	90
β/°	90.429(3)
γ/°	90
Volume/Å^3	911.90(12)
Z	2
ρ_{calc}g/cm^3	2.678
μ/mm^{-1}	4.191
F(000)	688.0
Crystal size/mm^3	0.21 × 0.17 × 0.1
Radiation	MoKα (λ = 0.71073)
2Θ range for data collection/°	6.458 to 56.702
Index ranges	$-8 \leq h \leq 8$, $-16 \leq k \leq 16$, $-15 \leq l \leq 15$
Reflections collected	6850
Independent reflections	2265 [R_{int} = 0.0194, R_{sigma} = 0.0232]
Data/restraints/parameters	2265/0/139
Goodness-of-fit on F^2	1.090
Final R indexes [I>=2σ (I)]	R_1 = 0.0234, wR_2 = 0.0561
Final R indexes [all data]	R_1 = 0.0286, wR_2 = 0.0590
Largest diff. peak/hole / e Å^{-3}	0.62/-1.19

Figure S5. Molecular structure and atom numbering scheme for $[Au\{Fe(CO)_5\}_2][HOB\{3,5\text{-}(CF_3)_2C_6H_3\}_3]$.

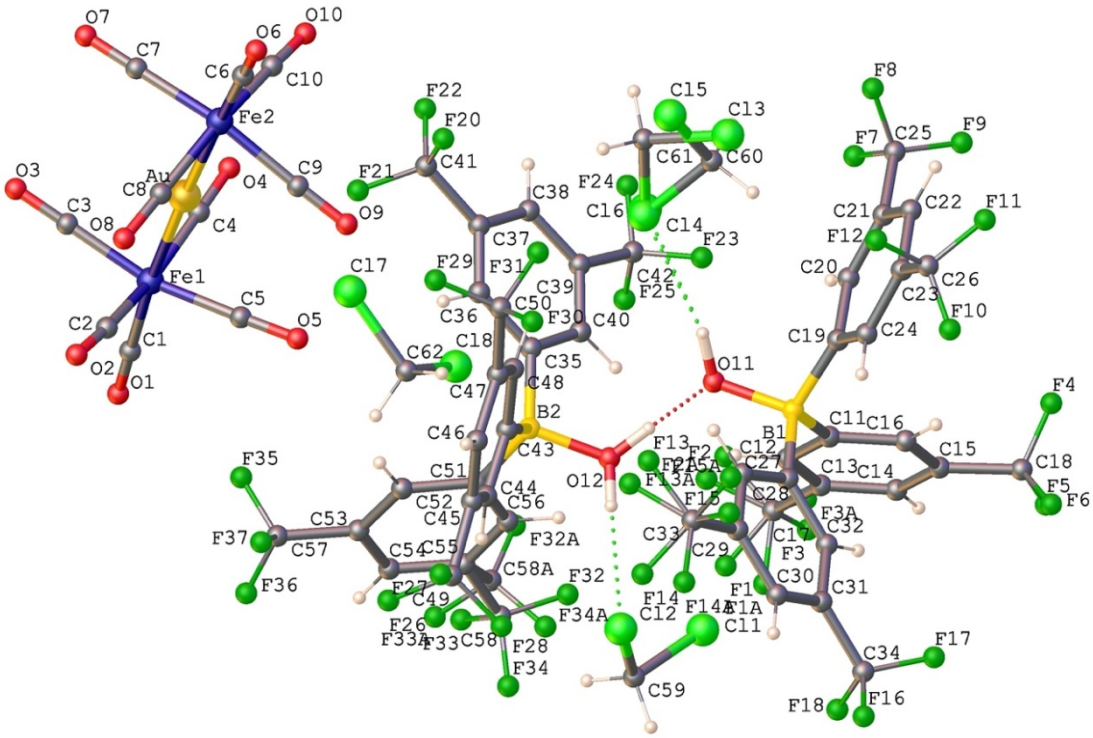

Table S5. Crystal data and structure refinement for $[Au\{Fe(CO)_5\}_2][HOB\{3,5-(CF_3)_2C_6H_3\}_3]\bullet [H_2OB\{3,5-(CF_3)_2C_6H_3\}_3]\bullet 2.5(CH_2Cl_2)$**.**

Identification code	Rad785
Empirical formula	$C_{60.5}H_{26}AuB_2Cl_5F_{36}Fe_2O_{12}$
Formula weight	2136.35
Temperature/K	100.0
Crystal system	monoclinic
Space group	$P2_1/n$
a/Å	12.7265(14)
b/Å	41.135(4)
c/Å	14.3567(15)
α/°	90
β/°	92.702(2)
γ/°	90
Volume/Å^3	7507.4(14)
Z	4
ρ_{calc}g/cm^3	1.890
μ/mm^{-1}	2.655
F(000)	4140.0
Crystal size/mm^3	0.48 × 0.35 × 0.05
Radiation	MoKα (λ = 0.71073)
2Θ range for data collection/°	4.626 to 54.968
Index ranges	$-16 \leq h \leq 16$, $-53 \leq k \leq 53$, $-18 \leq l \leq 18$
Reflections collected	140822
Independent reflections	17218 [R_{int} = 0.0717, R_{sigma} = 0.0424]
Data/restraints/parameters	17218/238/1203
Goodness-of-fit on F^2	1.226
Final R indexes [I>=2σ (I)]	R_1 = 0.0821, wR_2 = 0.1662
Final R indexes [all data]	R_1 = 0.0913, wR_2 = 0.1703
Largest diff. peak/hole / e Å^{-3}	1.62/-4.92

References

[1] a) Becke, A. D. *Phys. Rev. A* **1988**, *38*, 3098–3100; (b) Perdew, J. P. *Phys. Rev. B* **1986**, *33*, 8822–8824; (c) Grimme, S.; Ehrlich, S.; Goerigk, L. *J. Comput. Chem.* **2011**, *32*, 1456–1465; (d) Grimme, S.; Antony, J.: Ehrlich, S.; Krieg, H. *J. Chem. Phys.* **2010**, *132*, 154104; (e) Weigend, F.; Ahlrichs, R. *Phys. Chem. Chem. Phys.* **2005**, *7*, 3297–3305; (f) Weigend, F. *Phys. Chem. Chem. Phys.***2006**, *8*, 1057–1065.

[2] Gaussian 16, Revision A.03, Frisch, M. J. et al. Gaussian, Inc., Wallingford CT (2016).

[3] a) F. Weinhold, C. Landis, Valency and Bonding, A Natural Bond Orbital Donor – Acceptor Perspective, Cambridge University Press, Cambridge, 2005; b) C. R. Landis and F. Weinhold, "The NBO View of Chemical Bonding", in, G. Frenking and S. Shaik (eds.), The Chemical Bond: Fundamental Aspects of Chemical Bonding (Wiley, 2014), pp. 91-120.

[4] E. D. Glendening, C. R. Landis, F. Weinhold, J. Comput. Chem. 2013, 34, 1429.

[5] R. F. W. Bader,Atoms in Molecules: A Quantum Theory, 1990, Oxford: Clarendon Press.

[6] AIMAll (Version 17.11.14), T. A. Keith, TK Gristmill Software, Overland Park KS, USA, 2017.

[7] P. Pollak, F. Weigend, *J. Chem. Theory Comput.*, **2017**, *13*, 3696-3705.

[8] Ziegler, T.; Rauk, A. *Theor. Chim. Acta*, **1977**, *46*, 1–10.

[9] a) Mitoraj, M.; Michalak, A. *Organometallics* **2007**, *26*, 6576–6580; b) Mitoraj, M.; Michalak, A. *J. Mol. Model.* **2008**, *14*, 681–687.

[10] a) ADF2017, SCM, Theoretical Chemistry, Vrije Universiteit, Amsterdam, The Netherlands, http://www.scm.com; b) G. te Velde, F. M. Bickelhaupt, E. J. Baerends, C. F. Guerra, S. J. A. van Gisbergen, J. G. Snijders, T. Ziegler, *J. Comput. Chem.* **2001**, *22*, 931–967.

[11] a) E. van Lenthe, E. J. Baerends, *J. Comput. Chem*. **2003**, *24*, 1142-1156; b) E. van Lenthe, E. J. Baerends, J. G. Snijders, *J. Chem. Phys*. **1993**, *99*, 4597; c) E. van Lenthe, E. J. Baerends, J. G. Snijders, *J. Chem. Phys*. **1994**, *101*, 9783.

[12] a) G. Frenking, F. M. Bickelhaupt, *The Chemical Bond 1. Fundamental Aspects of Chemical Bonding*, chap. The EDA Perspective of Chemical Bonding, 121–158. Wiley-VCH: Weinheim (2014); b) L. Zhao, M. von Hopffgarten, D. M. Andrada, G. Frenking, *WIREs Comput. Mol. Sci.* **2018**, *8*, 1345; c) L. Zhao, M. Hermann, M.; W.H.E. Schwarz, G. Frenking, *Nat. Rev. Chem.* **2019**, *3*, 48-63; d) L. Zhao, S. Pan, N. Holzmann, P. Schwerdtfeger, G. Frenking, *Chem. Rev*. **2019**, *119*, 8781-8845.

[13] a) M. Fianchini, C. F. Campana, B. Chilukuri, T. R. Cundari, V. Petricek, H. V. R. Dias, *Organometallics* **2013**, *32*, 3034-3041; b) H. V. R. Dias, M. Fianchini, T. R. Cundari, C. F. Campana, *Angew. Chem., Int. Ed.* **2008**, *47*, 556-559.

[14] L. Krause, R. Herbst-Irmer, G. M. Sheldrick, D. Stalke, *J. Appl. Crystallogr*. **2015**, *48*, 3-10.

[15] G. M. Sheldrick, *Acta Crystallogr. Sect. A: Found. Adv*. **2015**, *71*, 3-8.

[16] G. M. Sheldrick, *Acta Crystallogr. Sect. C: Struct. Chem*. **2015**, *71*, 3-8.

[17] O. V. Dolomanov, L. J. Bourhis, R. J. Gildea, J. A. K. Howard, H. Puschmann, *J. Appl. Crystallogr.* **2009,** *42*, 339-341.